Onset of convection in the icy Galilean satellites: Influence of rheology

Amy C. Barr[1] and Robert T. Pappalardo

Laboratory for Atmospheric and Space Physics, University of Colorado, Boulder, Colorado, USA

Received 18 October 2004; revised 4 August 2005; accepted 10 August 2005; published 7 December 2005.

[1] Ice I exhibits a complex rheology at temperature and pressure conditions appropriate for the interiors of the ice I shells of Europa, Ganymede, and Callisto. We use numerical methods and existing parameterizations of the critical Rayleigh number to determine the conditions required to trigger convection in an ice I shell with each of the stress-, temperature- and grain size–dependent rheologies measured in laboratory experiments by Goldsby and Kohlstedt (2001). The critical Rayleigh number depends on the ice grain size and the amplitude and wavelength of temperature perturbation issued to an initially conductive ice I shell. If the shells have an assumed uniform grain size <0.4 mm, deformation during initial plume growth is accommodated by Newtonian volume diffusion. If the ice grain size is between 0.4 mm and 3 cm, deformation during plume growth is accommodated by weakly non-Newtonian grain boundary sliding, where the critical ice shell thickness for convection depends on the amplitude of temperature perturbation to the −0.5 power. If the ice grain size exceeds 2 cm, convection can not occur in the ice I shells of the Galilean satellites regardless of the amplitude or wavelength of temperature perturbation. If the grain size in a convecting ice I shell evolves to effective values greater than 2 cm, convection will cease. If the ice shell has a grain size large enough to permit flow by dislocation creep, the ice is too stiff to permit convection, even in the thickest possible ice I shell. Consideration of the complex ice rheology implies that estimates of the grain size in the satellites and knowledge of their initial thermal states are required when judging the convective instability of their ice I shells.

Citation: Barr, A. C., and R. T. Pappalardo (2005), Onset of convection in the icy Galilean satellites: Influence of rheology, *J. Geophys. Res.*, *110*, E12005, doi:10.1029/2004JE002371.

1. Introduction

[2] Measurements of the gravitational and magnetic fields of the Jovian satellites Europa, Ganymede, and Callisto suggest that these satellites have liquid water oceans beneath an outer layer of ice I [*Anderson et al.*, 1996, 1998, 2001; *Zimmer et al.*, 2000; *Kivelson et al.*, 2002]. The thickness of Europa's outer H_2O-rich layer is less than 170 km, but the relative thickness of the ice shell and potential subsurface liquid water ocean are uncertain [*Anderson et al.*, 1998]. In Ganymede and Callisto, the internal oceans are likely near depth of the ice I–III phase transition, which occurs at a depth of ~170 km, but the thicknesses of their oceans are unknown. The striking differences in the interior structures and surface morphologies of Europa, Ganymede, and Callisto [*Schubert et al.*, 2004; *Greeley et al.*, 2004; *Pappalardo et al.*, 2004; *Moore et al.*, 2004] suggest that differing roles of heat transport by solid-state convection and heat generation by tidal dissipation in each body may have led these three satellites down different evolutionary paths. Efforts to judge whether the outer ice I shells convect and to determine the likely role of convection in driving endogenic resurfacing have been limited by uncertainties in the ice I shell thicknesses, rheology of ice, and role of tidal dissipation.

[3] The stability of a basally heated fluid layer against convection can be judged by comparing the timescale for growth of Rayleigh-Taylor instabilities (convective plumes) at the base of the fluid layer to the thermal diffusion timescale, which controls the rate of decay of temperature fluctuations driving plume growth. The ratio of these timescales is expressed by the Rayleigh number,

$$Ra = \frac{\rho g \alpha \Delta T D^3}{\kappa \eta}, \quad (1)$$

where ρ is the density of the fluid, g is the acceleration of gravity, α is the coefficient of thermal expansion, ΔT is the temperature difference between the surface and bottom of the layer, D is the layer thickness, κ is the thermal diffusivity, and η is the fluid viscosity. Convection can occur in a fluid layer if the Rayleigh number exceeds a critical value, Ra_{cr}. The critical Rayleigh number for convection in any fluid depends on the wavelength of

[1]Now at Department of Earth and Planetary Sciences, Washington University in St. Louis, St. Louis, Missouri, USA.

0148-0227/05/2004JE002371$09.00

initial temperature perturbation issued to the layer and the geometry of the layer. For a fluid with a temperature-dependent viscosity, the critical Rayleigh number also depends on $\partial \ln(\eta)/\partial T$ [*Solomatov*, 1995].

[4] A large volume of work exists regarding the onset of convection in the ice I shells of the satellites assuming a Newtonian rheology, where the viscosity of ice is independent of stress. Early works such as that of *Reynolds and Cassen* [1979] approximated ice as a constant-viscosity fluid, and determined that convection could occur in an ice I shell on a Ganymede-like satellite if the shell was greater than ~30 km thick. Algebraic relationships between the activation energy in the ice flow law (which controls $\partial \ln(\eta)/\partial T$) and the critical Rayleigh number for a Newtonian fluid derived by *Solomatov* [1995] have been used to determine the conditions required to start convection in an ice shell with a temperature-dependent viscosity [e.g., *Pappalardo et al.*, 1998], and grain-size– and temperature-dependent viscosity [*McKinnon*, 1999]. Each of these studies yielded essentially the same conclusion: the critical shell thickness for convection in the ice I shells of the Galilean satellites was predicted to be ~20–30 km, depending on the rheological parameters used for ice.

[5] Laboratory experiments suggest that ice I exhibits a complex rheology at temperatures and stresses appropriate for a convecting ice shell in the icy Galilean satellites [*Goldsby and Kohlstedt*, 2001]. Analogous to minerals in the Earth's mantle, Newtonian volume diffusion accommodates deformation in ice for small grain sizes and/or high temperatures. At large grain sizes and/or large stresses, ice flows by strongly stress-dependent dislocation creep. For intermediate stresses and grain sizes, strain in ice I is accommodated by weakly stress-dependent grain boundary sliding (GBS) and basal slip. The resulting rheology for ice is Newtonian (independent of stress) when volume diffusion accommodates strain, and becomes increasingly non-Newtonian (stress-dependent) as the grain size of ice increases and/or the temperature decreases.

[6] If a layer of basally heated non-Newtonian fluid is in a conductive equilibrium, the viscosity of the motionless fluid is very large, and a finite-amplitude perturbation is required to soften the fluid sufficiently to permit convection. The critical Rayleigh number for convection in a non-Newtonian fluid therefore depends on the amplitude and wavelength of the initial buoyancy perturbation. The buoyancy perturbation could be compositional, similar to the instability of thickened continental lithosphere beneath continents on Earth [*Molnar et al.*, 1998], or thermal, such as the onset of tidal dissipation in an icy satellite [*Barr et al.*, 2004]. If a temperature perturbation is issued to the fluid layer, the critical Rayleigh number depends on the amplitude of thermal perturbation if this amplitude is less than the characteristic temperature difference that drives convection beneath the stagnant lid (the rheological temperature scale) [*Barr et al.*, 2004]. If the amplitude of the temperature perturbation issued to the fluid layer exceeds the rheological temperature scale, the critical Rayleigh number for convection does not depend on perturbation amplitude and achieves a constant minimum value.

[7] The most widely applied definition of the critical Rayleigh number for non-Newtonian, basally heated fluids comes from the work of *Solomatov* [1995], who developed an algebraic relationship between the stress exponent, activation energy, and the minimum critical Rayleigh number for convection in the limit of large initial temperature perturbations. The critical Rayleigh number calculated by *Solomatov* [1995] is directly relevant to terrestrial planets whose warm initial state post-accretion likely permits convection, which is maintained by radiogenic heating of their interiors.

[8] Applied to the icy satellites, the definition of critical Rayleigh number from *Solomatov* [1995] yields an absolute lower limit on the critical ice shell thickness required for convection, assuming that large lateral temperature perturbations of order ~40 K are present in the ice shell to trigger convection. The initial temperature states of the satellites' ice shells are not known. If the shells are close to the limit of convective stability, they may periodically reach a conductive equilibrium with radiogenic heating in their interiors, wherein lateral temperature perturbations available to start convection in the ice shell are very small. The convective stability of the ice shell then depends on the amplitudes and spatial distribution of temperature perturbations available to soften the ice.

[9] *Barr et al.* [2004] examined the convective stability of an initially conductive ice I shell under the influence of grain boundary sliding and basal slip. The critical Rayleigh number for convection in ice with a rheology of only GBS or only basal slip was found to obey a power law scaling with the amplitude of perturbation for amplitudes between 0.7 K and 17 K. In the limit of large amplitude perturbations (>37 K), the critical Rayleigh number was found to approach a constant, asymptotic value. *Barr et al.* [2004] concluded that convection could occur in the outer ice I layers of Europa, Ganymede, and Callisto provided stringent requirements on shell thickness, perturbation amplitude, and grain size are met simultaneously. If deformation in ice were accommodated by the GBS deformation mechanism alone, then convection in Europa, Ganymede, or Callisto could only occur in an ice shell with a grain size of 1 mm or less, triggered by a temperature perturbation of order 1 to 10 Kelvin in ice shells greater than 100 km thick.

[10] Grain boundary sliding and basal slip accommodate deformation in ice I near the base of an ice shell for a relatively limited range of grain sizes. For grain sizes smaller than ~1 mm, deformation near the base of the shell is accommodated by Newtonian volume diffusion, and for grain sizes greater than ~1 cm, deformation is accommodated by highly non-Newtonian dislocation creep. The role of dislocation creep and volume diffusion in accommodating convective strain during initial plume growth were left unaddressed by *Barr et al.* [2004]. Using similar numerical methods, we extend the results of that previous work to characterize the conditions required to trigger convection from a conductive equilibrium in an ice I shell where deformation is accommodated by volume diffusion, grain boundary sliding, or dislocation creep. We combine numerically determined values for Ra_{cr} for dislocation creep obtained in this study, existing numerical data on the critical Rayleigh number for GBS from *Barr et al.* [2004], and the results of *Solomatov* [1995] for volume diffusion to predict the conditions required to trigger convection in an

Table 1. Rheological Parameters[a]

Rheology	A (m^p Pa^{-n} s^{-1})	n	p	Q^* (kJ mol^{-1})
Volume diffusion[b]	1.2×10^{-10}	1	2	59.4
Basal slip	2.2×10^{-7}	2.4	0	60
Grain boundary sliding	6.2×10^{-14}	1.8	1.4	49
Dislocation creep	4.0×10^{-19}	4.0	0	60

[a]After *Goldsby and Kohlstedt* [2001].
[b]For T_m = 260 K.

ice shell with the laboratory-derived rheology of *Goldsby and Kohlstedt* [2001].

2. Rheology of Ice I

[11] The deformation mechanisms that accommodate large convective strains in the ice shells of the Galilean satellites, and the descriptive parameters in the ice flow law are by no means certain. In this study, we choose to explore how consideration of the multiple deformation mechanisms identified by *Goldsby and Kohlstedt* [2001] change the conditions required to trigger convection in the satellites.

[12] A large volume of experimental data and observations exists regarding the rheology of ice I in terrestrial and planetary contexts [*Durham and Stern*, 2001, and references therein]. Recent laboratory experiments seeking to clarify the deformation mechanisms responsible for flow in terrestrial ice sheets suggest that a composite flow law which includes terms due to diffusional flow, grain boundary sliding, basal slip, and dislocation creep [*Goldsby and Kohlstedt*, 2001] can match both viscosity measurements from terrestrial ice sheets [*Peltier et al.*, 2000] and previous laboratory experiments.

[13] The laboratory experiments of *Goldsby and Kohlstedt* [2001] suggest that deformation in ice I is accommodated by four creep mechanisms, resulting in a composite flow law:

$$\dot{\varepsilon}_{total} = \dot{\varepsilon}_{diff} + \dot{\varepsilon}_{disl} + \left(\frac{1}{\dot{\varepsilon}_{bs}} + \frac{1}{\dot{\varepsilon}_{GBS}}\right)^{-1}. \quad (2)$$

The composite flow law includes contributions from diffusional flow (*diff*), dislocation creep (*disl*), and grain-size-sensitive creep (GSS), where deformation occurs by both basal slip (*bs*) and grain boundary sliding (*GBS*) [*Goldsby and Kohlstedt*, 2001]. Basal slip and GBS are dependent mechanisms and both must operate simultaneously to permit deformation. When responsible for flow, the total strain rate for GSS is controlled by the slower of the two constituent mechanisms [*Durham and Stern*, 2001].

[14] The strain rate for each creep mechanism in the composite rheology (equation 2) is described by

$$\dot{\varepsilon} = A\frac{\sigma^n}{d^p}\exp\left(\frac{-Q^*}{RT}\right), \quad (3)$$

where $\dot{\varepsilon}$ is the strain rate, A is the pre-exponential parameter, σ is the differential stress, n is the stress exponent, d is the ice grain size, p is the grain size exponent, Q^* is the activation energy, R is the gas constant, and T is temperature. Governing parameters for GBS, basal slip, and dislocation creep derived from the laboratory experiments of *Goldsby and Kohlstedt* [2001] are summarized in Table 1.

[15] In ice with a small grain size (~0.1 mm) near its melting point, deformation is likely accommodated by diffusion creep, which occurs by both volume diffusion and grain boundary diffusion. Although diffusion creep has not been directly observed in laboratory measurements of ice rheology, *Goldsby and Kohlstedt* [2001] provide estimates of the governing parameters, which can be used to determine the strain rate from diffusion creep,

$$\dot{\varepsilon}_{diff} = \frac{42V_m\sigma}{3RT_m d^2}\left(D_v + \frac{\pi\delta}{d}D_b\right), \quad (4)$$

where V_m is the molar volume, T_m is the melting temperature of ice, D_v is the rate of volume diffusion, δ is the grain boundary width, and D_b is the rate of grain boundary diffusion [*Goldsby and Kohlstedt*, 2001]. Note that our definition of the strain rate from diffusion creep includes a factor of 3 that was inadvertently omitted from the definition in *Goldsby and Kohlstedt* [2001] (see *Goodman et al.* [1981] for a discussion). The grain sizes we consider are much larger than the grain boundary width ($\delta \sim 9.04 \times 10^{-10}$ m) [*Goldsby and Kohlstedt*, 2001], so volume diffusion dominates over grain boundary diffusion, and we may ignore the contribution of grain boundary diffusion to the strain rate. The strain rate for volume diffusion alone is

$$\dot{\varepsilon}_{diff} = \frac{A_{diff}}{d^2}D_{o,v}\exp\left(\frac{-Q_v^*}{RT}\right), \quad (5)$$

where $D_{o,v}$ is the volume diffusion rate coefficient and Q_v^* is the activation energy. Volume diffusion is Newtonian, but the viscosity does depend on grain size. The parameters for volume diffusion are listed in Table 1, where we have grouped the pre-exponential parameters to calculate an effective $A_{diff} = (42V_mD_{o,v}/3RT_m)$.

[16] The laboratory experiments of *Goldsby and Kohlstedt* [2001] are performed for smaller grain sizes than values used in our study (3–200 microns), as well as higher temperatures (170–268 K) and higher stresses (0.2–20 MPa). Their empirical fits to the laboratory data are used to extrapolate the flow laws to conditions appropriate for the interiors of the ice I shells of the satellites, namely, grain sizes of 50 microns to 10 cm, temperatures between 90 and 260 K, and stresses between 10^{-4} and 0.1 MPa.

[17] *Goldsby and Kohlstedt* [2001] provide an alternate set of creep parameters for GBS and dislocation creep for ice near its melting point. For $T > 255$ K, deformation rates in ice due to GBS are increased by a factor of 1000, in response to melting at grain boundaries and edges, resulting in very low viscosities near the melting point. A similar effect occurs for dislocation creep at $T > 258$ K. We have not included the high temperature creep enhancement in our initial numerical models. Use of the creep enhancement for warm ice alone will result in extremely low viscosities near the base of the ice shell, which presents a difficulty for our numerical model.

[18] The vertical viscosity structure near the base of the ice shell controls the viscous restoring forces that retard

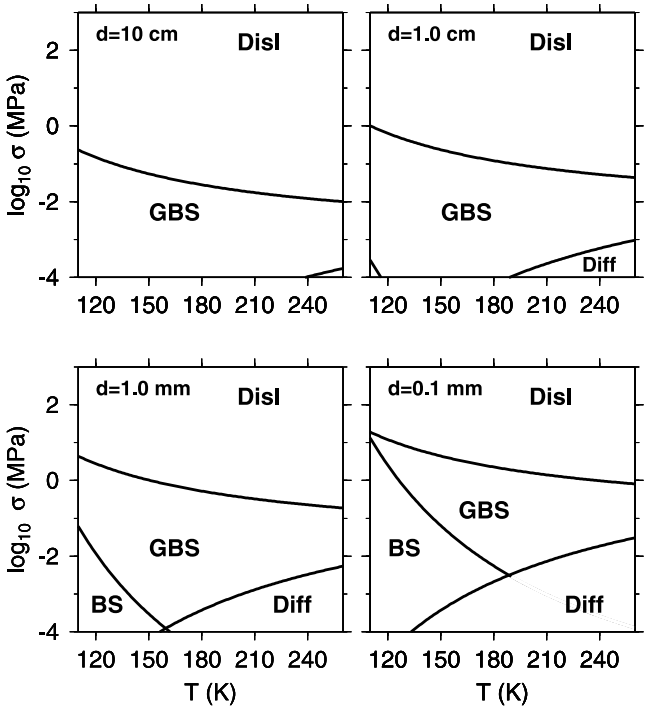

Figure 1. Deformation maps for ice I using the rheology of *Goldsby and Kohlstedt* [2001], for ice with grain sizes of 10 cm, 1.0 cm, 1.0 mm, and 0.1 mm. Lines on the maps represent the transition stress between deformation mechanisms as a function of temperature. A melting temperature of 260 K is assumed. For large grain sizes, dislocation creep (Disl, $n = 4$) dominates the rheological behavior for thermal stresses associated with initial plume growth in the icy satellites ($\sim 10^{-4}$–10^{-2} MPa). The weakly non-Newtonian deformation mechanisms grain boundary sliding (GBS, $n = 1.8$), and basal slip (BS, $n = 2.4$) play important roles for intermediate grain sizes (1.0 cm and 1.0 mm). Diffusional flow (Diff), which is a Newtonian deformation mechanism, becomes important at small stresses, small grain sizes, and temperatures close to the melting point.

growth of initial convective plumes, so estimates of the grain size near the melting point of ice are useful for evaluating the conditions required to permit convection. The grain sizes of ice in the satellites are not well constrained, with estimates spanning 8 orders of magnitude, from microns [*Nimmo and Manga*, 2002] to meters [*Schmidt and Dahl-Jensen*, 2004]. Terrestrial ice sheets under similar stress and temperature conditions as the base of Europa's ice shell exhibit grain sizes of order 1–5 mm [*De La Chapelle et al.*, 1998]. Grain growth in Europa's ice shell would be limited by rapid tidal flexing of the ice shell and by the presence of non-water-ice materials [*McKinnon*, 1999]. The presence of non-water-ice materials in the shells of Ganymede and Callisto might similarly limit grain growth in these satellites as well. To account for the uncertainty in the grain size of ice within the icy Galilean satellites, we characterize the conditions required for convection as a function of grain size. We also assume that the ice shells have a uniform grain size, which is implausible in a real ice shell.

[19] The deformation mechanism that yields the largest strain rate for a given temperature and differential stress is inferred to accommodate deformation in ice at that temperature and stress level. The transition stress between any pair of flow laws, for example, GBS and dislocation creep, is described by

$$\sigma_T = \left[\frac{A_{GBS}}{A_{disl}}\frac{d^{p_{disl}}}{d^{p_{GBS}}}\exp\left(\frac{(Q^*_{disl} - Q^*_{GBS})}{RT}\right)\right]^{\frac{1}{n_{disl}-n_{GBS}}}. \quad (6)$$

The expressions for the transition stresses between the various deformation mechanisms can be used to construct deformation maps showing the boundaries of regimes of dominance for each constituent creep mechanism. Deformation maps for ice with grain sizes 0.1 mm, 1.0 mm, 1.0 cm, and 10 cm are illustrated in Figure 1.

[20] The non-Newtonian deformation mechanisms will accommodate the strain due to growth of initial convective plumes if the thermal stress generated by the plume exceeds the transition stress between diffusional flow and GSS/dislocation creep. The thermal stress due to a plume of height λ, warmer than its surroundings by δT, is approximately $\sigma_{th} \sim \rho g \alpha \delta T \lambda$. In an ice shell 50 km thick on Europa, Ganymede, or Callisto, a plume with height $\lambda \sim D$ and $\delta T \sim 5$ K can generate a thermal stress of $\sim$0.03 MPa. In an ice shell 25 km thick, a plume of height approximately 25 km can generate $\sim$0.015 MPa. Note that the estimates of thermal stresses from a growing plume are significantly higher than the thermal stresses that drive flow in the warm sublayer of an actively convecting ice shell ($\sim 10^{-3}$ MPa [*Tobie et al.*, 2003]) because convection can only occur in the ice shell if the growing plume generates enough stress to overcome the viscous restoring force from the overlying cold ice.

[21] At the melting temperature of ice, the transition stress between GBS and diffusional flow in ice with a grain size of 1.0 mm is 0.02 MPa. If the ice grain size is 0.1 mm, the transition stress increases to 0.1 MPa; with a grain size of 100 mm, the transition stress is only 6×10^{-4} MPa. Therefore it is plausible that GBS accommodates the strain from initial plume growth in ice with a grain size close to 1 mm. Similarly, at the melting temperature of ice, the transition stress between GBS and dislocation creep in ice with a grain size of 10 cm is 10^{-4} MPa, so it is plausible that dislocation creep accommodates convective strain during the onset of convection in ice with a grain size of order 10 cm. At the temperatures ($T > 180$ K) and stresses ($\sigma \sim 10^{-4}$–10^{-1} MPa) relevant to the onset of convection in the ice shells, basal slip does not play an appreciable role in accommodating deformation (see Figure 1), and its role is neglected in our analysis.

3. Numerical Experiments

[22] An effective viscosity can be calculated from the strain rates due to each individual creep mechanism as

$$\eta_{eff} = \frac{\sigma}{2\dot{\varepsilon}_{II}}, \quad (7)$$

Table 2. Thermal and Physical Parameters

Parameter	Symbol	Value
Density of ice	ρ	930 kg m^{-3}
Acceleration of gravity	g	1.3 m s^{-2}
Coefficient of thermal expansion	α	10^{-4} K^{-1}
Surface temperature	T_s	90–120 K
Melting temperature	T_m	260 K
Thermal diffusivity	κ	10^{-6} m s^{-2}
Thermal conductivity	k	3.3 W m^{-1} K^{-1}
Gas constant	R	8.314 J mol^{-1} K^{-1}

where σ is the effective shear stress, and $\dot{\varepsilon}_{II}$ is the second invariant of the strain rate tensor. We use an explicit strain rate-dependent rheology of form

$$\eta = \left(\frac{d^p}{2A}\right)^{(1/n)} \dot{\varepsilon}_{II}^{(1-n)/n} \exp\left(\frac{Q^*}{nRT}\right), \tag{8}$$

where $\dot{\varepsilon}_{II}$ is the second invariant of the strain rate tensor. Values of the rheological parameters are taken directly from the lab-derived flow laws of [*Goldsby and Kohlstedt*, 2001] and are summarized in Table 1.

[23] The dynamics of thermal convection are controlled by the Rayleigh number, a single dimensionless parameter that expresses the ratio between the timescale of plume growth at the base of the fluid layer and the thermal diffusion timescale. Large values of *Ra* indicate vigorous convection; convection cannot occur unless the Rayleigh number exceeds the critical Rayleigh number (Ra_{cr}). We define a reference Rayleigh number for the ice shell as [*Barr et al.*, 2004]

$$Ra_1 = \frac{\rho g \alpha \Delta T D^{(n+2)/n}}{\left(\kappa d^p (2A)^{-1}\right)^{1/n} \exp\left(\frac{Q^*}{nRT_m}\right)}, \tag{9}$$

where ρ is the density of ice, g is the acceleration of gravity, ΔT is the temperature difference between the surface of the convecting layer (T_s) and the melting temperature of ice (T_m), D is the thickness of the convecting layer, κ is the thermal diffusivity, d is the grain size of ice, A is the pre-exponential parameter, n is the stress exponent, and R is the gas constant. The reference Rayleigh number (9) is obtained from the traditional definition (equation (1)) of the thermal Rayleigh number by explicitly evaluating the non-Newtonian viscosity of ice at a reference strain rate $\dot{\varepsilon}_{II,o} = \kappa/D^2$ and the melting temperature of ice ($T = T_m$).

[24] We have implemented a non-Newtonian rheology for ice I in the finite element convection model Citcom [*Moresi and Gurnis*, 1996; *Zhong et al.*, 1998, 2000; *Barr et al.*, 2004], which solves the governing equations of thermally driven convection in an incompressible fluid. Our simulations are run in 2D Cartesian geometry. Free-slip boundary conditions are used on the surface ($z = 0$), base ($z = -D$), and edges ($x = 0$, x_{max}) of the domain. The simulations used to characterize the behavior of dislocation creep in this study are performed in a domain with 64 × 64 elements, chosen to resolve the bottom thermal boundary layer while allowing sufficient coverage of our large parameter space given limited computational resources. Increasing the numerical resolution from 32 × 32 elements as used by *Barr et al.* [2004] to 64 × 64 elements decreases the value of Ra_{cr} by 5%. We use a higher resolution in this study compared to *Barr et al.* [2004] to allow numerical stability of solutions with somewhat larger stress exponents and perturbation amplitudes. To ensure numerical stability, we also impose an upper viscosity cutoff of $\eta_{max} = 10^{10}\ \eta_o$.

[25] The layer is purely basally heated, so internal heating by tidal dissipation is not considered. However, tidal heating may play a role in triggering convection in the icy satellites by generating finite-amplitude temperature perturbations to soften the ice [*Barr et al.*, 2004], and potentially by modifying the viscosity and grain size of the ice shell [*McKinnon*, 1999], which we discuss in section 6. We explore how Ra_{cr} varies for a range of surface temperatures of the ice shell between 90 and 120 K, appropriate for the temperate and equatorial surfaces of the Jovian icy satellites. We have not taken into account the thermal or rheological effects of contaminant non-water-ice materials such as hydrated sulfuric acid, or hydrated sulfate salts, which have been suggested to exist on the surfaces of the satellites on the basis of near-infrared spectroscopy [*McCord et al.*, 1999; *Carlson et al.*, 1999]. Values of thermal and physical parameters are summarized in Table 2.

[26] The approach we use to numerically determine the critical Rayleigh number is similar to linear stability analysis [*Turcotte and Schubert*, 1982; *Chandrasekhar*, 1961]. The convection simulations are started from an initial condition of a conductive ice shell plus a temperature perturbation expressed as a single Fourier mode,

$$T(x,z) = T_s - \frac{z\Delta T}{D} + \delta T \cos\left(\frac{2\pi D}{\lambda} x\right) \sin\left(\frac{-z\pi}{D}\right), \tag{10}$$

where δT and λ are the amplitude and wavelength of the temperature perturbation, and $z = -D$ at the warm base of the ice shell. Use of free-slip boundary conditions requires that the width of the computational domain (x_{max}) be equal to one half the wavelength of initial perturbation. Because the critical Rayleigh number is a function of both the wavelength and amplitude of temperature perturbation, we first determine the value of wavelength that minimizes the value of Ra_{cr} for $\delta T = 0.05\ \Delta T$, then investigate how Ra_{cr} for the specific Fourier mode with $\lambda = \lambda_{cr}$ varies with δT.

[27] The dimensionless kinetic energy of the fluid layer is used as a diagnostic for the vigor of convection. The dimensionless kinetic energy is defined by

$$E = \frac{\int_0^{x_{max}} \int_0^D \left(v_x^2 + v_z^2\right) dx dz}{\int_0^{x_{max}} \int_0^D dx dz}, \tag{11}$$

where $x_{max} = \lambda/(2D)$ is the width of the numerical domain, and v_x and v_z are the horizontal and vertical fluid velocities, respectively. If the kinetic energy of the fluid grows with time during the opening stages of the simulation, the layer is judged to convect; if the kinetic energy decays with time, the layer does not convect and the system returns to conductive equilibrium. During initial plume growth in a non-Newtonian fluid, the kinetic energy increases super-exponentially owing to the feedback between the increasing convective velocities and strain rate-dependent viscosity

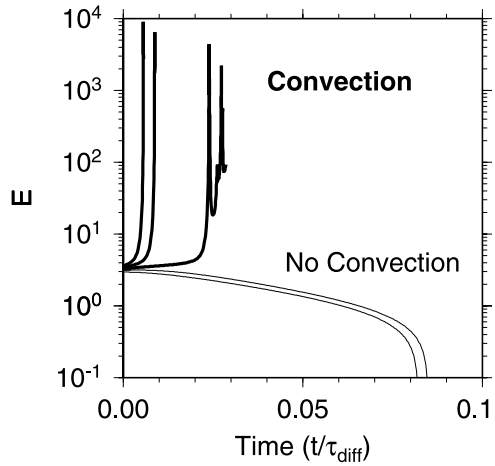

Figure 2. Growth or decay of dimensionless kinetic energy (E) with nondimensional time ($t' = t/\tau_{diff}$ where the thermal diffusion time $\tau_{diff} = \kappa/D^2$) for a series of ice convection simulations with dislocation creep rheology. Each curve represents the evolution of kinetic energy for a simulation with a different Rayleigh number ranging from $Ra_1 = 1.4 \times 10^4$ (top curve) to $Ra_1 = 1.0 \times 10^4$ (bottom curve). The kinetic energy grows super-exponentially in simulations where convection occurs (thick lines), and decays in simulations where convection does not occur (thin lines).

[*Molnar et al.*, 1998; *Barr et al.*, 2004]. A family of curves illustrating the growth of kinetic energy in ice deforming by dislocation creep is illustrated in Figure 2. For a given initial condition, we run a series of convection simulations with decreasing values of Ra_1. The critical Rayleigh number is defined as the minimum value of Ra_1 where the system convects for a given initial condition, and here is determined to two significant figures.

4. Results

[28] To estimate the conditions required to trigger convection in an ice shell with a composite rheology, we first determine the critical Rayleigh number for convection in a fluid where deformation is accommodated by a single microphysical mechanism, then combine this information to predict the stability criterion of an ice shell where all three deformation mechanisms operate simultaneously. As discussed in section 2, basal slip does not play an appreciable role in accommodating deformation during the onset of convection. When grain boundary sliding and basal slip operate simultaneously near the base of an ice shell (where $T \sim T_m$), grain boundary sliding is the rate-limiting mechanism [*Barr et al.*, 2004]. First, we characterize the critical Rayleigh number as a function of wavelength and perturbation amplitude for dislocation creep, and compare our numerical results to the critical Rayleigh number predicted by *Solomatov* [1995] in the limit of large perturbation amplitudes. We then summarize the results of *Barr et al.* [2004] that describe the variation in critical Rayleigh number for GBS as a function of perturbation amplitude and wavelength. Finally, we estimate the critical Rayleigh number for convection and corresponding critical wavelength for Newtonian volume diffusion using the results of *Solomatov* [1995] and *Stengel et al.* [1982].

4.1. Dislocation Creep

[29] On the basis of the results of *Barr et al.* [2004], we expect the critical Rayleigh number for convection in ice with a solely dislocation creep rheology to depend on a power of the amplitude of temperature perturbation for perturbations smaller than the rheological temperature scale. We call this regime of behavior the "power law" regime. For perturbations larger than the rheological temperature scale [*Solomatov and Moresi*, 2000],

$$\Delta T_{rh} = \frac{1.2(n+1)RT_i^2}{Q^*\Delta T}, \tag{12}$$

where T_i is the roughly isothermal temperature beneath the stagnant lid, we expect the critical Rayleigh number to reach a minimum constant value. We call this regime of behavior the "asymptotic" regime. Using the activation energy for dislocation creep and the nominal set of boundary temperatures in our study (T_s = 110 K and T_m = 260 K), the value of ΔT_{rh} is approximately 0.375 $\Delta T \sim$ 56 K if $T_i \sim T_m$ = 260 K.

[30] Regardless of the rheology of the convecting fluid, the critical Rayleigh number depends on the wavelength of perturbation issued to the fluid layer [*Chandrasekhar*, 1961; *Turcotte and Schubert*, 1982]. The wavelength that minimizes Ra_{cr} for dislocation creep is $\lambda_{cr} \sim 1.45D$. Figure 3 illustrates the variation in critical Rayleigh number as a function of wavelength for T_s = 110 K and T_m = 260 K, for a temperature perturbation of amplitude 7.5 K. The critical Rayleigh number varies by a factor of 1.5 as the wavelength is varied from 1.2D to 2.4D. Consistent with the results of *Barr et al.* [2004], we find that the critical Rayleigh number is weakly dependent on wavelength in the asymptotic regime, varying by 10% as λ is increased from 1.5D to 3.0D. To within the precision of our experiments, 2.0D < λ_{cr} < 2.6D in the asymptotic regime.

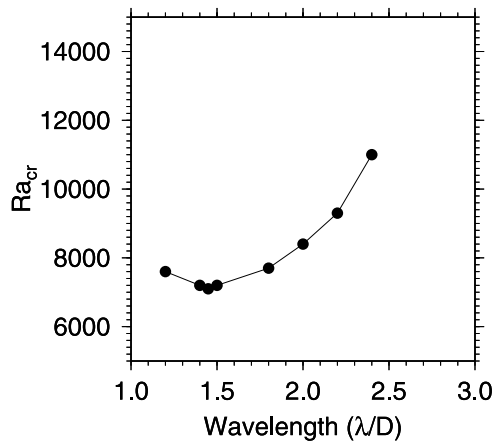

Figure 3. Critical Rayleigh number as a function of wavelength for ice with dislocation creep rheology. A constant temperature perturbation of 7.5 K is used. The critical Rayleigh number varies by ~20% as λ is varied from 1.2D to 2.4D. The minimum value of $Ra_{cr} = 7.1 \times 10^3$ occurs at a $\lambda \sim 1.45D$.

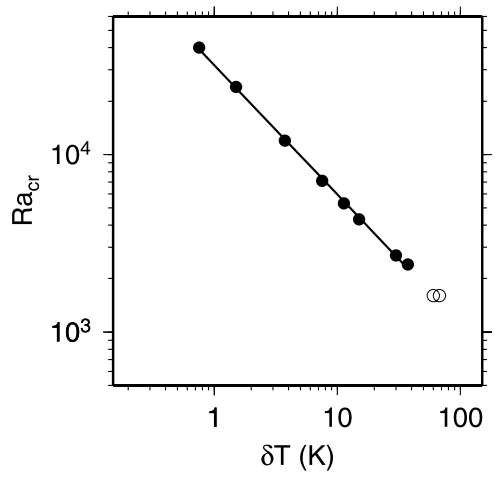

Figure 4. Critical Rayleigh number for convection in ice with dislocation creep rheology as a function of perturbation amplitude (δT) for small-amplitude perturbations (solid circles) and perturbations larger than the rheological temperature scale (open circles). For $\delta T < \Delta T_{rh}$, the critical Rayleigh number varies as a power of the perturbation amplitude. For $\delta T \geq \Delta T_{rh}$, the critical Rayleigh number achieves a constant asymptotic value of 1.6×10^3. The line indicates a least squares fit to the data, where the fitting coefficient θ in equation (13) is equal to 0.727.

[31] In the power law regime, the critical Rayleigh number obeys a relationship of form [*Barr et al.*, 2004]

$$Ra_{cr} = Ra_a \left(\frac{\delta T}{\Delta T_{rh}} \right)^{-\theta}, \tag{13}$$

where Ra_a is the numerically determined value of the critical Rayleigh number in the asymptotic regime. Use of ΔT_{rh} in the scaling relationship promotes a simple interpretation of the coefficient Ra_a as the asymptotic minimum value of Rayleigh number characterized by *Solomatov* [1995]. Values of θ are obtained using a least squares fit to values of Ra_{cr} as a function of δT in log-log space. Figure 4 illustrates the variation in critical Rayleigh number as a function of perturbation amplitude for dislocation creep for T_s = 110 K and T_m = 260 K. For these boundary temperatures, we find $Ra_a = 1.6 \times 10^3$ and $\theta = 0.727$. Values of Ra_a and θ obtained for 90 K < T_s < 120 K creep are summarized in Table 4 in section 4.3. Consistent with results from our previous work, we find that changing the assumed melting temperature of the ice shell by 10 K has a minimal effect on the value of Ra_a. However, varying the surface temperature between 90 K and 120 K causes the value of Ra_a to change by a factor of $\sim$1.5.

[32] To compare our numerically derived values of Ra_a for dislocation creep to the value of Ra_a predicted by *Solomatov* [1995], we employ the algebraic relationship between Ra_a, activation energy, and stress exponent derived by *Barr et al.* [2004]. Because the numerical data obtained in this study uses an Arrhenius temperature dependence rather than a temperature-linearized flow law, *Barr et al.* [2004] suggested a slight correction to the relationship between activation energy and Ra_a derived by *Solomatov* [1995].

[33] Using this correction, the asymptotic Rayleigh number is related to the stress exponent and activation energy by

$$Ra_a = Ra_{cr}(n) \left(\frac{z_{\max}}{D} \right)^{-2(n+1)/n} \exp\left(\frac{E}{1 - \frac{z_{\max}}{2D} + T'_o} - \frac{E}{1 + T'_o} \right), \tag{14}$$

where $z_{\max}$ is given by

$$z_{\max} = \frac{D}{2(n+1)} \left(4(n+1)\left(T'_o + 1\right) + En - \left(8En(n+1)\left(T'_o + 1\right) + E^2 n^2 \right) \right)^{1/2}, \tag{15}$$

with $T'_o = T_s/\Delta T$, and $E = Q^*/nR\Delta T$ [*Barr et al.*, 2004]. The value of $Ra_{cr}(n)$, which represents the critical Rayleigh number for convection in a fluid with a solely stress-dependent viscosity, is given by

$$Ra_{cr}(n) = Ra_{cr}(1)^{1/n} Ra_{cr}(\infty)^{(n-1)/n}, \tag{16}$$

where $Ra_{cr}(1) = 1568$ and $Ra_{cr}(\infty) \sim 20$ [*Solomatov*, 1995]. The values obtained using these expressions for dislocation creep and our numerically derived values for Ra_a are summarized in Table 3. Similar to results from our previous study, the numerical values of Ra_a and those predicted by the analysis of *Solomatov* [1995] agree to within $\sim$5–25%, depending on the surface temperature.

[34] If the shell is in the stagnant lid regime, the thickness of the warm sublayer ($z_{\max}$) is a small fraction of the ice shell of thickness (D). In the warm sublayer beneath the stagnant lid, the temperature is approximately constant and the viscosity of the ice depends solely on stress. The criteria for convective stability in the sublayer can therefore be expressed in terms of the thickness of the warm sublayer and the critical Rayleigh number for convection in a fluid with a stress-dependent (but not temperature-dependent) viscosity [*Solomatov*, 1995].

[35] The analysis of *Solomatov* [1995] and *Barr et al.* [2004] applies only when the ice shell is in the stagnant lid regime and convective instability first sets in at the base of the shell. This implies that the thickness of the warm isothermal sublayer is much smaller than the thickness of the total ice shell, or $z_{\max}/D \ll 1$. Using rheological parameters appropriate for dislocation creep and the nominal upper and lower boundary temperatures of 110 K and 260 K, $z_{\max}/D \sim 0.75$ for the dislocation creep rheology. Some of the disagreement between our numerically derived values of Ra_a and values obtained from equations (14) and (15) may arise because the ice shell is close to the boundary between the sluggish lid and stagnant lid convective regimes [*Solomatov*, 1995].

Table 3. Comparison of Ra_a Values for Dislocation Creep to Values Predicted by *Solomatov* [1995]

T_s (K)	T_m (K)	This Study	*Solomatov* [1995]
90	260	2.4×10^3	2.1×10^3
100	260	2.0×10^3	1.8×10^3
110	260	1.6×10^3	1.5×10^3
120	260	1.6×10^3	1.3×10^3

Table 4. Summary of Ra_a and θ Values

Rheology	T_s (K)	Ra_a	θ
Volume diffusion	90	3.64×10^6	0
	100	2.86×10^6	0
	110	2.21×10^6	0
	120	1.67×10^6	0
Grain boundary sliding	90	3.1×10^4	0.492
	100	2.7×10^4	0.486
	110	2.2×10^4	0.467
	120	1.9×10^4	0.469
Dislocation creep	90	2.4×10^3	0.729
	100	2.0×10^3	0.746
	110	1.6×10^3	0.727
	120	1.6×10^3	0.742

[36] Additionally, because convection actually occurs in our simulations when $Ra_1 = Ra_{cr}$, our simulations place an upper bound on the value of Ra_{cr}. The true value may be up to 10% lower than the values reported here, because we determine Ra_{cr} to two significant figures only.

4.2. Grain Boundary Sliding

[37] Using methods identical to those described in section 3, *Barr et al.* [2004] considered the critical Rayleigh number for convection in an ice shell with deformation accommodated by solely grain boundary sliding. The inferred Ra_{cr} values were found to obey a scaling relationship between perturbation amplitude and an asymptotic value similar to equation (13). The critical wavelength for the GBS rheology was found to be $1.5D$ in the power law regime and $\sim 2.0D$ in the asymptotic regime. Asymptotic values of Rayleigh number and values of the power θ for GBS with 90 K < T_s < 120 K are summarized in Table 4. The rheological temperature scale for GBS with T_s = 110 K and T_m = 260 K is approximately 40 K. Values of the asymptotic Rayleigh number for $\delta T > 40$ K match values predicted by equations (14) and (15) to within 35–60% depending on the value of surface temperature [*Barr et al.*, 2004].

4.3. Volume Diffusion

[38] The critical Rayleigh number for volume diffusion can be estimated using equation (14), with $n = 1$,

$$Ra_{cr} = 1568\left(\frac{z_{\max}}{D}\right)^{-4} \exp\left(\frac{E}{1 - \frac{z_{\max}}{2D} + T'_o} - \frac{E}{1 + T'_o}\right), \qquad (17)$$

where $z_{\max}$ is given by

$$z_{\max} = \frac{D}{4}\left(8\left(T'_o + 1\right) + E - \left(16E\left(T'_o + 1\right) + E^2\right)\right)^{1/2}. \qquad (18)$$

The critical Rayleigh number for volume diffusion with T_s = 110 K and T_m = 260 K is 2.2×10^6, and varies by a factor of ~1.5 as a function of surface temperature. Values for Ra_{cr} for 90 K < T_s < 120 K are summarized in Table 4. The critical wavelength for convection in volume diffusion can be estimated using the algebraic relationship between the critical wavelength and activation energy derived by *Stengel et al.* [1982],

$$\lambda_{cr} = \frac{16}{p}, \qquad (19)$$

where $p = (Q^*\Delta T)/(RT_i^2)$ is the Frank-Kamenetskii parameter [*Solomatov*, 1995]. Using T_s = 110 K and $T_i \sim T_m$ = 260 K, and the activation energy for volume diffusion, p = 15.8, yielding an estimate of $\lambda_{cr} \sim D$.

5. Critical Ice Shell Thickness

[39] Using the definition of the Rayleigh number, and the values of critical Rayleigh number, we first determine the critical ice shell thickness for convection in an ice shell assuming deformation is accommodated by each individual term in the *Goldsby and Kohlstedt* [2001] flow law. The critical ice shell thickness curves are then combined to predict how the critical shell thickness for convection varies as a function of perturbation amplitude and grain size in an ice shell where deformation is accommodated simultaneously by volume diffusion, GBS, and dislocation creep.

5.1. Single Rheology

[40] The critical shell thickness for convection in an ice shell with deformation accommodated by a single flow law is given by [*Barr et al.*, 2004]

$$D_{cr} = \left(\frac{Ra_{cr}\left(\kappa d^p (2A)^{-1}\right)^{1/n} \exp\left(\frac{Q^*}{nRT_m}\right)}{\rho g \alpha \Delta T}\right)^{n/(n+2)}. \qquad (20)$$

If plume growth is accommodated by GBS or dislocation creep, the critical ice shell thickness is a function of perturbation amplitude (δT) and grain size (d), for perturbation amplitudes less than 40 K for GBS and less than 56 K for dislocation creep. For perturbations larger than the rheological temperature scale, the critical Rayleigh number reaches a minimum, constant value, D_a,

$$D_a = \left(\frac{Ra_a\left(\kappa d^p (2A)^{-1}\right)^{1/n} \exp\left(\frac{Q^*}{nRT_m}\right)}{\rho g \alpha \Delta T}\right)^{n/(n+2)}, \qquad (21)$$

where Ra_a is the asymptotic value of critical Rayleigh number. If Newtonian volume diffusion controls plume growth, Ra_{cr} is independent of perturbation amplitude.

[41] Figure 5 summarizes the critical ice shell thickness for convection as a function of grain size in an ice shell where deformation is accommodated solely by volume diffusion, grain boundary sliding, or dislocation creep, for small (0.75 K), modest (7.5 K), and large amplitude ($\delta T >$ 56 K) temperature perturbations. For volume diffusion, $D_{cr} \propto d^{2/3}$ because the viscosity of ice depends on grain size squared, while for GBS, $D_{cr} \propto d^{1.4/3.8}$. If plume growth were accommodated by solely dislocation creep, the critical ice shell thickness would not depend on d because the viscosity of the ice is independent of grain size.

[42] We note that *Ruiz* [2001] suggested that convection could not occur in the ice I shells of the satellites if deformation was accommodated by the non-Newtonian deformation mechanisms grain boundary sliding or dislocation creep, regardless of the amplitude of temperature perturbation issued to the ice shells. However, subsequent works regarding convection in Europa [*Nimmo and Manga*, 2002; *Barr et al.*, 2004] suggest that the outer ice I shells of

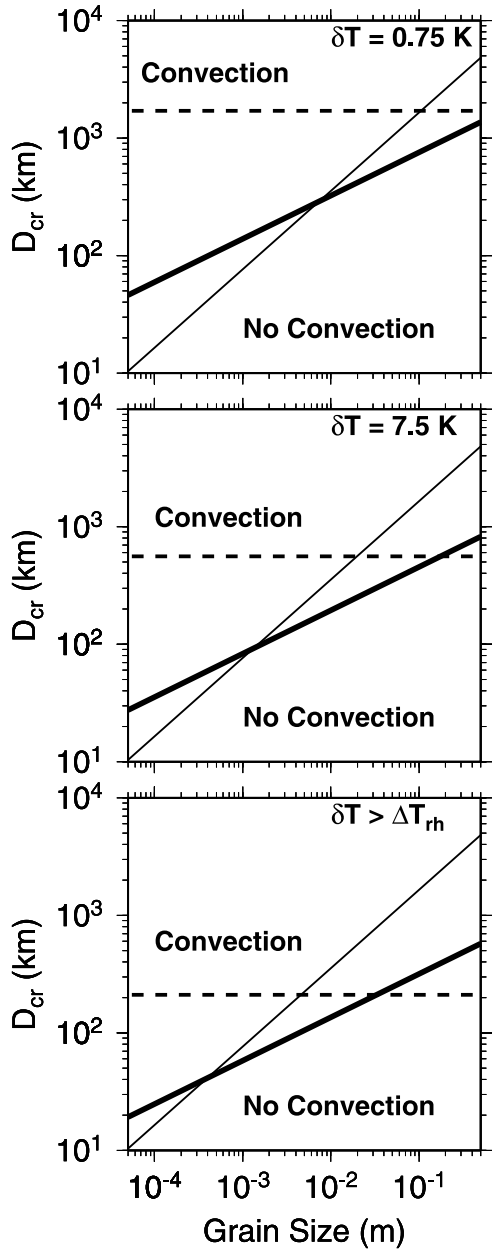

Figure 5. Critical ice shell thickness (D_{cr}) for convection as a function of grain size for (top) $\delta T = 0.75$ K, (middle) $\delta T = 7.5$ K, and (bottom) $\delta T > \Delta T_{rh}$ for dislocation creep (56 K). Assuming that deformation in the ice shell is accommodated by either volume diffusion (thin line) or GBS (thick line), D_{cr} depends on grain size because the viscosities for these mechanisms depend on grain size. For dislocation creep (dashed line), D_{cr} is independent of grain size, and is larger than the maximum permitted ice I shell thickness in the icy Galilean satellites, regardless of temperature perturbation.

the satellites can convect, even if deformation is accommodated by the non-Newtonian mechanisms. The essential geophysical argument in both this study and in *Ruiz* [2001] is to compare the Rayleigh number at the base of an ice shell to the critical Rayleigh number for convection. The values of critical Rayleigh number for dislocation creep and GBS used by *Ruiz* [2001] are obtained using the results of *Solomatov* [1995], and therefore are similar to the values of Ra_a obtained from our numerical results. However, we find that a mathematical discrepancy exists between the viscosity function used by *Solomatov* [1995] and the viscosity function used by *Ruiz* [2001], which resulted in *Ruiz* [2001] calculating values of Ra_1 for Callisto's ice shell that were several orders of magnitude lower than the values predicted by the nominal definition of Rayleigh number for a non-Newtonian fluid (equation (9)). The temperature-linearized flow law described in equation (7) of *Solomatov* [1995] uses a nondimensionalized temperature (where $T = 1$ at the base of the ice shell), but the analysis by *Ruiz* [2001] appears to treat this temperature as dimensionalized (where $T = T_m$ in Kelvin at the base of the ice shell). Figure 6 illustrates Ra_1 as a function of ice shell thickness using equation (9) compared to the values of Ra_1 predicted by Figure 1 of *Ruiz* [2001]. If the mathematical error in the analysis of *Ruiz* [2001] is corrected, our results are similar

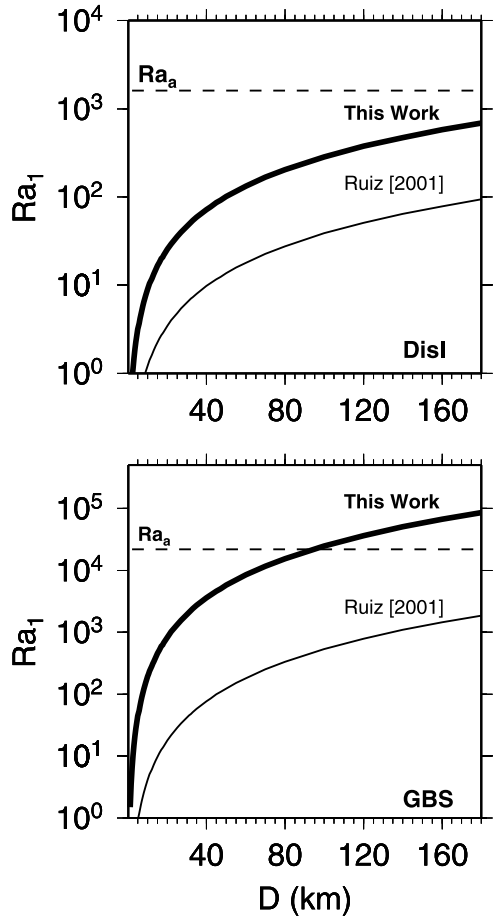

Figure 6. Comparison of Rayleigh number at the base of the ice shell (Ra_1) from our study (thick line) with values obtained by *Ruiz* [2001] (thin line) for (top) dislocation creep and (bottom) GBS. Convection can occur if Ra_1 exceeds the critical Rayleigh number (Ra_a, dashed line). A discrepancy between the flow law used by *Solomatov* [1995] and the flow law adopted by *Ruiz* [2001] incorrectly resulted in critical ice shell thicknesses for convection much larger than the maximum permitted shell thickness.

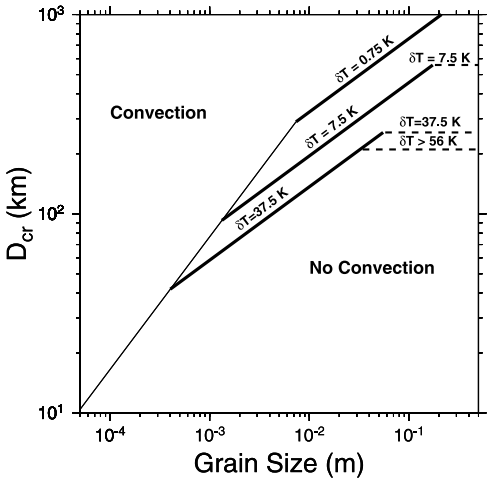

Figure 7. Critical ice shell thickness (D_{cr}) for convection in a multi-rheology ice shell as a function grain size for δT = 0.75 K, δT = 7.5 K, and δT = 37.5 K, and in the limit of $\delta T \geq \Delta T_{rh}$. For the nominal boundary temperatures, ΔT_{rh} = 37.5 K for GBS and 56 K for dislocation creep. The value of D_{cr} for a composite-rheology ice shell is the minimum value of D_{cr} predicted by each constituent rheology (see Figure 5). For δT = 7.5 K, deformation is accommodated by volume diffusion (thin line) when the grain size of the ice shell is less than 1 mm. If δT = 7.5 K, GBS (thick line) accommodates deformation when the grain size is between than 1 mm and 2 cm. For a smaller δT, volume diffusion accommodate strain during plume growth for a wider range of grain sizes. For a larger δT, GBS and dislocation creep (dashed line) dominate over volume diffusion for a wider range of grain sizes. For a grain size greater than 2 cm, the minimum shell thickness required for convection in the limit of $\delta T > 56$ K exceeds the maximum permitted ice I shell thickness in the icy Galilean satellites. Because dislocation creep would accommodate strain from plume growth only in very thick ice shells with grain sizes larger than 2 cm, it does not play a role in controlling plume growth in the icy Galilean satellites.

in the limit of large amplitude temperature perturbations (i.e., in the asymptotic regime).

5.2. Composite Rheology

[43] In an ice shell where volume diffusion, GBS, and dislocation creep accommodate strain simultaneously, deformation due to plume growth at the base of the ice shell will be accommodated by the mechanism that predicts the largest strain rate (equivalently, the smallest viscosity) in the active sublayer near the base of the ice shell. To first order, the stability criterion for the active sublayer of the ice shell, and therefore the entire ice shell [*Solomatov*, 1995] should be governed by the single deformation mechanism that predicts the largest strain rates at the base of the ice shell. Therefore the actual governing parameters of the rheology (namely, the stress exponent and $\partial \ln(\eta)/\partial T$, which control Ra_{cr}) in the warm sublayer of a composite-rheology ice shell should be close to the values predicted by a single flow law. Each constituent rheology predicts a different value of Ra_{cr} (i.e., $Ra_{cr,\ diff}$, $Ra_{cr,\ GBS}$, $Ra_{cr,disl}$), and convection will occur when $Ra_{1,diff} > Ra_{cr,diff}$, $Ra_{1,GBS} > Ra_{cr,diff}$, or $Ra_{1,disl} > Ra_{cr,disl}$. The critical ice shell thickness for convection is therefore defined as the minimum value of D where Ra_1 exceeds Ra_{cr} for any single rheology, or

$$D_{cr,composite} = \min\left(D_{cr,diff}, D_{cr,GBS}, D_{cr,disl}\right). \tag{22}$$

[44] If the stress due to a growing thermal plume is close to the grain size- and temperature-dependent transition stress between two deformation mechanisms, the deformation at the base of the shell would be accommodated by multiple deformation mechanisms, and the actual governing parameters that control the value of Ra_{cr} could represent an amalgamation of the governing parameters of each constituent rheology. In that case, equation (22) would provide only a crude estimate of the value of Ra_{cr} for the ice shell.

[45] Figure 7 summarizes the critical shell thickness for convection under the composite rheology for perturbation amplitudes δT of 0.75 K, 7.5 K, 37.5 K, and $\delta T > 56$ K. For small grain sizes and small perturbation amplitudes, volume diffusion accommodates deformation during plume growth. As the perturbation amplitude increases, the stress in the ice shell due to the thermal plume increases, allowing the non-Newtonian deformation mechanisms GBS and dislocation creep to become active. Therefore the deformation mechanism controlling flow during the onset of convection is a function of perturbation amplitude. Because the transition stress between volume diffusion and the non-Newtonian deformation mechanisms decreases as grain size increases, the thermal stress due to initial plume growth is sufficient to activate the non-Newtonian deformation mechanisms for large grain sizes. Therefore the roles of GBS and dislocation creep in accommodating strain during plume growth increase as the grain size of the ice shell increases. The wavelength of the fastest growing convective plumes (λ_{cr}) changes for each deformation mechanism. The value of critical wavelength is $\lambda_{cr} \sim D$ for volume diffusion, $\lambda_{cr} \sim 1.5D$ for GBS, and $\lambda_{cr} \sim 1.45D$ for dislocation creep. We report the minimum ice shell thickness for convection as a function of perturbation amplitude for each grain size, assuming that the temperature perturbation always has $\lambda = \lambda_{cr}$ for the individual deformation mechanism that controls flow at that grain size and δT. Therefore our D_{cr} values are minimum values where convection can occur given the ice grain size and temperature perturbation issued to the shell.

[46] For a given pair of deformation mechanisms, the grain size where one mechanism begins to dominate over the other can be calculated by equating the expressions for D_{cr} for each rheology. The transition grain size d_t is a function of the activation energies, stress exponents, and grain size exponents for the flow laws, and the amplitude of temperature perturbation,

$$d_t(\delta T) = \left(\frac{C_i}{C_j}\right)^{\gamma}, \tag{23}$$

where

$$\gamma = \frac{1}{\frac{p_j}{(n_j+2)} - \frac{p_i}{(n_i+2)}} \tag{24}$$

and $n_{i,j}$ are the stress exponents for each flow law, and $p_{i,j}$ are the grain size exponents. The values of C for each flow

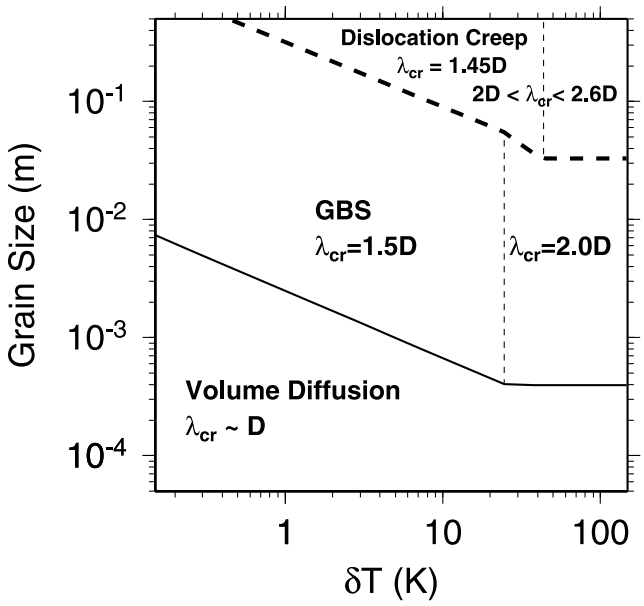

Figure 8. Transition grain size between plume growth accommodated by volume diffusion versus GBS (thin) and GBS versus dislocation creep (dashed) as a function of temperature perturbation δT. For $\delta T > 56$ K, volume diffusion controls plume growth for grain sizes less than 0.4 mm, GBS controls plume growth for grain sizes between 0.4 mm and 3 cm, and dislocation creep controls plume growth for grain sizes greater than 3 cm. For a smaller δT, for example, 0.75 K, volume diffusion accommodates strain for larger grain sizes, up to 7 mm. Values of the critical wavelength for each rheology are shown for the power law (small δT) and asymptotic (large δT) regimes.

law are derived from the definition of the Rayleigh number (equation (9)) and are given by

$$C_i = \left[\frac{Ra_{a,i} \left(\frac{\delta T}{\Delta T_{rh,i}} \right)^{-\theta_i} \exp\left(\frac{Q^*}{n_i R T_m} \right) \left(\kappa (2A_i)^{-1} \right)^{1/n_i}}{\rho g \alpha \Delta T} \right]^{n_i/(n_i+2)}, \quad (25)$$

where A, Q^*, n, Ra_a, ΔT_{rh}, θ, are dependent on the rheology, and Ra_a, θ, ΔT are additionally dependent on the boundary temperatures (T_s and T_m).

[47] Figure 8 illustrates the variation in transition grain size between volume diffusion, GBS, and dislocation creep as a function of perturbation amplitude, for T_s = 110 K and T_m = 260 K. In the limit of large temperature perturbations ($\delta T > 56$ K), strain during plume growth is accommodated by volume diffusion for grain sizes less than 0.4 mm, by GBS for 0.4 mm < d < 3.2 cm, and by dislocation creep for $d > 3.2$ cm. For a smaller perturbation amplitude, for example δT = 7.5 K, the transition between volume diffusion and GBS occurs at a grain size of 1.3 mm, and the transition from GBS to dislocation creep occurs at a grain size of 17 cm.

6. Implications for the Icy Galilean Satellites

[48] Gravity and magnetic data returned by the Galileo spacecraft suggest that Europa, Ganymede, and Callisto have internal oceans, but the portion of their outer H_2O layers that are solid is not well constrained. The maximum thickness of Europa's ice-rich layer is approximately 170 km [*Anderson et al.*, 1998], but estimates based on geological observations suggest that the solid ice shell is perhaps 20–25 km thick [*Pappalardo et al.*, 1999; *Nimmo et al.*, 2003]. For Ganymede and Callisto, the upper bound on ice I shell thickness is obtained by estimating the depth to the minimum melting point of ice I in each satellite. In Ganymede, assuming the shell is pure water ice with a density of 930 kg m^{-3}, the minimum melting point occurs at a depth of 160 km; in Callisto, 180 km. Depending on the present heat flux from their interiors, the ice shells of Ganymede and Callisto could be thinner.

[49] The flow law used here is specific to pure water ice, so important caveats are required before directly applying these results to the icy Galilean satellites. If impurities such as hydrated sulfuric acids, hydrated magnesium salts, or ammonia are present in the ice shells, the conditions for convection outlined here may not directly apply to the Galilean satellites. Deviation in the rheological parameters due to the presence of these or other materials could dramatically alter the rheology and the conditions required to initiate convection. Additionally, we have assumed a uniform grain size for the ice in the shells, which is an oversimplification. We have ignored internal heating by tidal dissipation, which is not well parameterized, in favor of exploring the interesting changes in behavior with grain size.

[50] We have not considered the temperature-dependence of the thermal conductivity (k) of ice. The temperature-dependent thermal conductivity modifies the temperature gradient in the ice shell, which could affect the value of Ra_{cr} by changing the value of $\partial \ln(\eta)/\partial T$ near the base of the shell. Additionally, the temperature-dependent conductivity changes the equivalent heat flow (F) out of the ice shell ($F = k\Delta T/D$). The effect of the temperature-dependent conductivity can be estimated by equating the heat flux across a constant-conductivity ice shell to the heat flux across a shell with a variable conductivity [*McKinnon*, 1999],

$$\frac{D_{true}}{D_{cr}} = \frac{621}{k_c \Delta T} \ln\left(\frac{T_m}{T_s} \right), \quad (26)$$

where D_{true} is the actual critical ice shell thickness with variable conductivity taken into account, D_{cr} is the value obtained assuming a constant thermal conductivity, and k_c is the constant value of thermal conductivity used in the definition of the Rayleigh number (3.3 W m^{-1} K^{-1}). The thermal conductivity is assumed to vary as a function of temperature as $621/T$ W m^{-1} [*Petrenko and Whitworth*, 1999]. For T_m = 260 K and T_s = 110 K, $D_{true}/D_{cr} \sim 1.08$, indicating that if a temperature-dependent thermal conductivity were used, the value of D_{cr} would be ~10% larger than values calculated here. The uncertainty in the ice rheology likely outweighs this effect, so we do not include it in our models at this time.

[51] We do not include the alternate set of rheological parameters presented by *Goldsby and Kohlstedt* [2001] for enhanced creep rates in ice near its melting point. If this effect is included, viscosities due to grain boundary sliding and dislocation creep are decreased because melting at grain

boundaries and grain edges permits faster creep for a given applied stress. If the high temperature creep enhancement were included in the numerical model, the viscosities near the base of the ice shell for grain sizes greater than 1.0 mm would be greatly reduced, potentially permitting convection in thinner ice shells than determined in this study. If the convective temperature of an ice shell is within several degrees of the melting point, the entire sublayer of the ice shell would then convect vigorously because of its low viscosity. Additionally, if tidal dissipation warmed the sublayer of an initially conductive ice shell to a temperature close to the melting point, the sublayer of the shell could have a viscosity low enough to become convectively unstable. Therefore an ice shell judged to be stable against convection in this study might be able to convect if the high temperature creep enhancement were included in the model. For this reason, it would be valuable to include this high temperature creep enhancement in future modeling efforts.

[52] Figure 7 shows the critical ice shell thickness for convection in Europa, Ganymede, and Callisto as a function of grain size. The value of $g = 1.3$ m s^{-2}, midway between the values for Ganymede and Callisto and appropriate to Europa, is used to generate the D_{cr} curve. Values of D_{cr} obtained using the values of g for Ganymede are smaller by 10%, and values obtained using g for Callisto are greater by 10%.

[53] For small grain sizes, $\leq$0.4 mm, Newtonian volume diffusion controls plume growth during the onset of convection. The critical ice shell thickness is between 10 and 40 km, and does not depend on the amplitude of temperature perturbation. The critical ice shell thickness increases as $d^{2/3}$.

[54] For intermediate grain sizes, between 0.4 mm and $\sim$1 cm, GBS controls plume growth if the temperature perturbation is sufficiently large. If δT = 37.5 K, GBS controls plume growth if the grain size is greater than 0.4 mm. If a smaller δT is issued to the ice shell, plume growth will be accommodated by volume diffusion. When GBS accommodates strain during the onset of convection, the critical ice shell thickness depends on the perturbation amplitude to the -0.5 power for $\delta T < 40$ K. For $\delta T > 40$ K, the critical shell thickness achieves a minimum value that is independent of perturbation amplitude. If GBS controls plume growth, the critical shell thickness depends on $d^{1.4/3.8}$.

[55] For large grain sizes, greater than 2 cm, the minimum critical ice shell thickness exceeds the maximum permitted ice I shell thickness in the icy Galilean satellites of 170 km, in the limit of perturbations greater than 56 K, for the nominal boundary temperatures. Dislocation creep accommodates deformation only for grain sizes larger than $\sim$3 cm, where the minimum shell thickness for convection is much greater than the maximum permitted shell thickness. Therefore dislocation creep does not play a role in controlling the growth of initial convective plumes in the satellites.

[56] Under the composite rheology, an ice shell with a nominally accepted shell thickness of Europa of 20–25 km [*Pappalardo et al.*, 1999; *Nimmo et al.*, 2003] can only convect if the ice grain size is less than 0.15–0.2 mm. If convection occurs in an ice shell 20–25 km thick on Europa, plume growth should be accommodated by Newtonian volume diffusion, and the grain size must be smaller than estimates based on terrestrial ice cores under similar temperature and strain rate conditions [*McKinnon*, 1999].

[57] If the ice shells of Ganymede and Callisto are in conductive equilibrium with present-day radiogenic heating (4.5×10^{-12} W kg^{-1} [*Spohn and Schubert*, 2003]) in their interiors, the equilibrium ice shell thicknesses are $\sim$130 km and $\sim$150 km, respectively. Convection can start from a modest temperature perturbation of 15 K in the present-day shell of Ganymede if the ice grain size is less than 5 mm. Strain during initial plume growth would be accommodated by GBS. If the perturbation amplitude exceeds the rheological temperature scale, the maximum grain size where convection can occur increases to 9 mm. Likewise, convection can start from a conductive equilibrium in Callisto's ice shell for $\delta T = 15$ K if the grain size is less than 7.5 mm; if $\delta T >$ 40 K, the maximum grain size for convection is 1.6 cm.

[58] The minimum asymptotic values of Rayleigh number also predict when convection will cease in an ice I shell. If the Rayleigh number of the ice shell drops below the asymptotic value, convection will stop. The Rayleigh number of the shell could decrease if the viscosity of the ice shell increases owing to grain growth, so if the grain size at the base of a convecting ice shell exceeds 2 cm, convection may cease. Tidal dissipation could also decrease the Rayleigh number of the shell if the tidal heat flux exceeds the maximum heat flux from convection, and the ice shell thins.

[59] Tidal dissipation may be able to generate the few Kelvin to tens of Kelvins temperature perturbations used as initial conditions in this study. Estimates have been made of the total amount of energy dissipated by tidal flexing of Europa and Ganymede's ice shells [*Murray and Dermott*, 1999; *Showman and Malhotra*, 1997], but the spatial distribution of the dissipation in their ice shells is not understood. It has been suggested that tidal dissipation is spatially localized within convective upwellings on length scales similar to the thickness of the ice shell in convective upwellings [*Tobie et al.*, 2003], or along zones of weakness in the ice shell [*Nimmo and Gaidos*, 2002; *Tobie et al.*, 2004]. If so, the critical Rayleigh number for tidally triggered convection would be similar to the values calculated here. It is also possible that the spatial pattern of tidal dissipation within an ice shell follows the spatial distribution of the tidal strain rate [*Ojakangas and Stevenson*, 1989]. In this case, the wavelength of tidal dissipation is much greater than the thickness of the ice shell, and much larger than the critical wavelength used in our calculation. For wavelengths larger or smaller than the critical wavelength, the value of critical Rayleigh number is higher, and the critical shell thickness for convection would be larger. Once the temperature perturbation due to tidal dissipation reaches the rheological temperature scale, the critical Rayleigh number approaches a constant asymptotic value. Therefore adding additional tidal heat would not trigger convection in the ice shell and could instead result in melting at the base of the shell and thinning of the shell. Regardless of the spatial distribution of tidal dissipation in the ice shells, tidal heating would likely concentrate itself near the warm base of the ice shell, promoting plume growth.

[60] We have assumed a uniform grain size for the ice shell, which is certainly an oversimplification. Tidal heating, rapid tidal flexing of the ice shells, and large convective

strains likely modify the size and orientation of ice grains in the shell. By analogy with terrestrial ice sheets, ice shelves, and the Earth's mantle, a complex suite of processes is likely to occur within the ice shells to cause grain sizes to evolve as a function of temperature, strain rate, impurity concentration, and total accumulated strain. For example, flow by dislocation creep is likely to lead to smaller grain sizes, whereas flow by grain boundary sliding or diffusional flow is likely to lead to grain growth [*De Bresser et al.*, 1998]. If grain growth or destruction occurs in ice, the change in grain size may cause the rate-limiting deformation mechanism to change as a function of the accumulated convective strain. Conclusions regarding the convective stability of the ice shells drawn from this study are strongly dependent on the ice grain size. Therefore we advocate using a more realistic grain size model in future work, by allowing grain size to dynamically evolve as a function of depth, temperature, stress and accumulated convective strain.

7. Summary and Conclusions

[61] Laboratory experiments suggest that ice I exhibits a complex rheological behavior at the temperatures and pressures appropriate to the interiors of the icy Galilean satellites. We find that the behavior of an ice I shell during the onset of convection is correspondingly complex. Under nominal conditions, growth of initial convective plumes at the base of the ice I shells of the icy Galilean satellites generates sufficient stress to activate both volume diffusion and grain boundary sliding. Therefore plume growth by both GBS and volume diffusion must be considered when judging the convective stability of the ice I shells.

[62] For small grain sizes ($d \leq 0.4$ mm), deformation is accommodated by volume diffusion. In this case, the conditions required for convection to start from a conductive equilibrium (i.e., Ra_{cr} and thus, D_{cr}) are independent of perturbation amplitude, depend on the wavelength of perturbation, minimize at $\lambda \sim D$, and depend on the grain size of the ice as $d^{2/3}$.

[63] For intermediate grain sizes (0.4 mm $< d <$ 3 cm), grain boundary sliding accommodates deformation during plume growth. For this range of grain sizes, the thermal stress associated with growing convective plumes is sufficient to drive flow by grain boundary sliding. In the limit of large temperature perturbations $\delta T > \Delta T_{rh}$ ($\sim$40 K for the nominal boundary temperatures considered here), GBS dominates the rheology if $d > 0.4$ mm. For smaller perturbations, the transition grain size increases to $\sim$0.7 mm for $\delta T < 1$ K.

[64] When GBS controls flow and $d < 2$ cm, convection can occur from a conductive equilibrium provided stringent requirements on the ice grain size, as well as the amplitude and wavelength of initial temperature perturbation, are met simultaneously. For small amplitude temperature perturbations, the critical Rayleigh number and ice shell thickness depend on the ratio of perturbation amplitude to the rheological temperature scale to the -0.5 power. If a large amplitude perturbation is issued to the shell ($\delta T > \Delta T_{rh}$), Ra_{cr} and D_{cr} achieve a constant minimum value.

[65] For large grain sizes ($d > 2$ cm), the ice is too stiff to permit convection in the satellites, regardless of the amplitude, wavelength, or source of buoyancy perturbation. Dislocation creep accommodates plume growth during the onset of convection if the ice grain size is >3 cm, but the viscosity of the ice is too high to permit convection. Therefore dislocation creep does not play a key role in plume growth during the onset of convection in the icy Galilean satellites.

[66] Convection can only occur if the grain size of ice is small enough to permit deformation by volume diffusion or GBS. Additionally, if the grain size of an actively convecting ice shell dynamically evolves to values greater than 2 cm, convection will cease. It may be difficult for tidal dissipation to trigger convection in a purely conductive ice shell under the current models of dissipation in the ice shells because preexisting temperature heterogeneities are required to focus tidal heating on short length scales.

[67] Consideration of the complex Newtonian/non-Newtonian rheology for ice I has highlighted several effects which must be included when judging convective stability. The grain size of ice controls both the conditions required to initiate convection and the conditions under which convection can continue. Small grain sizes (less than 1 mm) favor convection in the ice shell, and large grain sizes (greater than 2 cm) will not permit convection. The spatial distribution of temperature fluctuations in an initially conductive ice shell also affect the conditions required for convection. Temperature excesses of order a few to tens of Kelvin are required to start convection from a conductive equilibrium, and are most efficient at starting convection if they are distributed on wavelengths similar to the thickness of the ice shell. Consideration of the initial thermal state and the grain size distribution of an ice shell is necessary when judging whether convection occurs, and therefore how it affects the thermal evolution of an icy satellite.

[68] **Acknowledgments.** Support for this work is provided by NASA Graduate Student Researchers Program grant NGT5-50337 and NASA Exobiology grant NCC2-1340. This paper has benefited from work with Shijie Zhong, and helpful discussions with Allen McNamara, Bill McKinnon, and Slava Solomatov.

References

Anderson, J. D., E. L. Lau, W. L. Sjogren, G. Schubert, and W. B. Moore (1996), Gravitational constraints on the internal structure of Ganymede, *Nature*, *384*, 541–543.

Anderson, J. D., G. Schubert, R. A. Jacobson, E. L. Lau, W. B. Moore, and W. L. Sjogren (1998), Europa's differentiated internal structure: Inferences from four Galileo encounters, *Science*, *281*, 2019–2022.

Anderson, J. D., R. A. Jacobson, T. P. McElrath, W. B. Moore, G. Schubert, and P. C. Thomas (2001), Shape, mean radius, gravity field, and interior structure of Callisto, *Icarus*, *153*, 157–161.

Barr, A. C., R. T. Pappalardo, and S. Zhong (2004), Convective instability in ice I with non-Newtonian rheology: Application to the icy Galilean satellites, *J. Geophys. Res.*, *109*, E12008, doi:10.1029/2004JE002296.

Carlson, R. W., R. E. Johnson, and M. S. Anderson (1999), Sulfuric acid on Europa and the radiolytic sulfur cycle, *Science*, *286*, 97–99.

Chandrasekhar, S. (1961), *Hydrodynamic and Hydromagnetic Stability*, *Int. Ser. Monogr. Phys*, Clarendon, Oxford, U. K.

De Bresser, J. H. P., C. J. Peach, J. P. J. Reijs, and C. J. Spiers (1998), On dynamic recrystallization during solid state flow: Effects of stress and temperature, *Geophys. Res. Lett.*, *25*, 3457–3460.

De La Chapelle, S., O. Castelnau, V. Lipenkov, and P. Duval (1998), Dynamic recrystallization and texture development in ice as revealed by the study of deep ice cores in Antarctica and Greenland, *J. Geophys. Res.*, *103*, 5091–5106.

Durham, W. B., and L. A. Stern (2001), Rheological properties of water ice—Applications to satellites of the outer planets, *Annu. Rev. Earth Planet Sci.*, *29*, 295–330.

Goldsby, D. L., and D. L. Kohlstedt (2001), Superplastic deformation of ice: Experimental observations, *J. Geophys. Res.*, *106*, 11,017–11,030.

Goodman, D. J., H. J. Frost, and M. F. Ashby (1981), The plasticity of polycrystalline ice, *Philos. Mag. A*, *43*, 665–695.

Greeley, R. C., C. Chyba, J. W. Head, T. McCord, W. B. McKinnon, and R. T. Pappalardo (2004), Geology of Europa, in *Jupiter: The Planet, Satellites and Magnetosphere*, pp. 329–362, Cambridge Univ. Press, New York.

Kivelson, M. G., K. K. Khurana, and M. Volwerk (2002), The permanent and inductive magnetic moments of Ganymede, *Icarus*, *157*, 507–522.

McCord, T. B., et al. (1999), Hydrated salt minerals on Europa's surface from the Galileo near-infrared mapping spectrometer (NIMS) investigation, *J. Geophys. Res.*, *104*, 11,827–11,852.

McKinnon, W. B. (1999), Convective instability in Europa's floating ice shell, *Geophys. Res. Lett.*, *26*, 951–954.

Molnar, P., G. A. Houseman, and C. P. Conrad (1998), Rayleigh-Taylor instability and convective thinning of mechanically thickened lithosphere: Effects of non-linear viscosity decreasing exponentially with depth and of horizontal shortening of the layer, *Geophys. J. Int.*, *133*, 568–584.

Moore, J. M., et al. (2004), Callisto, in *Jupiter: The Planet, Satellites and Magnetosphere*, pp. 397–426, Cambridge Univ. Press, New York.

Moresi, L., and M. Gurnis (1996), Constraints on the lateral strength of slabs from three-dimensional dynamic flow models, *Earth Planet. Sci. Lett.*, *138*, 15–28.

Murray, C. D., and S. F. Dermott (1999), *Solar System Dynamics*, Cambridge Univ. Press, New York.

Nimmo, F., and E. Gaidos (2002), Strike-slip motion and double ridge formation on Europa, *J. Geophys. Res.*, *107*(E4), 5021, doi:10.1029/2000JE001476.

Nimmo, F., and M. Manga (2002), Causes, characteristics, and consequences of convective diapirism on Europa, *Geophys. Res. Lett.*, *29*(23), 2109, doi:10.1029/2002GL015754.

Nimmo, F., B. Giese, and R. T. Pappalardo (2003), Estimates of Europa's ice shell thickness from elastically-supported topography, *Geophys. Res. Lett.*, *30*(5), 1233, doi:10.1029/2002GL016660.

Ojakangas, G. W., and D. J. Stevenson (1989), Thermal state of an ice shell on Europa, *Icarus*, *81*, 220–241.

Pappalardo, R. T., et al. (1998), Geological evidence for solid-state convection in Europa's ice shell, *Nature*, *391*, 365–368.

Pappalardo, R. T., et al. (1999), Does Europa have a subsurface ocean? Evaluation of the geological evidence, *J. Geophys. Res.*, *104*, 24,015–24,056.

Pappalardo, R. T., G. C. Collins, J. W. Head, P. Helfenstein, T. McCord, J. M. Moore, L. M. Prockter, P. M. Schenk, and J. R. Spencer (2004), Geology of Ganymede, in *Jupiter: The Planet, Satellites and Magnetosphere*, pp. 363–396, Cambridge Univ. Press, New York.

Peltier, W. R., D. L. Goldsby, D. L. Kohlstedt, and L. Tarasov (2000), Ice-age ice-sheet rheology: constraints from the Last Glacial Maximum form of the Laurentide ice sheet, *Ann. Glaciol.*, *30*, 163–176.

Petrenko, V. F., and R. W. Whitworth (1999), *Physics of Ice*, Oxford Univ. Press, New York.

Reynolds, R. T., and P. M. Cassen (1979), On the internal structure of the major satellites of the outer planets, *Geophys. Res. Lett.*, *6*, 121–124.

Ruiz, J. (2001), The stability against freezing of an internal liquid-water ocean in Callisto, *Nature*, *412*, 409–411.

Schmidt, K. G., and D. Dahl-Jensen (2004), An ice crystal model for Jupiter's moon Europa, *Ann. Glaciol.*, *37*, 129–133.

Schubert, G., J. D. Anderson, T. Spohn, and W. B. McKinnon (2004), Interior composition, structure and dynamics of the Galilean satellites, in *Jupiter: The Planet, Satellites and Magnetosphere*, pp. 281–306, Cambridge Univ. Press, New York.

Showman, A. P., and R. Malhotra (1997), Tidal evolution into the Laplace resonance and the resurfacing of Ganymede, *Icarus*, *127*, 93–111.

Solomatov, V. S. (1995), Scaling of temperature- and stress-dependent viscosity convection, *Phys. Fluids*, *7*, 266–274.

Solomatov, V. S., and L.-N. Moresi (2000), Scaling of time-dependent stagnant lid convection: Application to small-scale convection on Earth and other terrestrial planets, *J. Geophys. Res.*, *105*, 21,795–21,818.

Spohn, T., and G. Schubert (2003), Oceans in the icy Galilean satellites of Jupiter?, *Icarus*, *161*, 456–467.

Stengel, K. C., D. C. Oliver, and J. R. Booker (1982), Onset of convection in a variable viscosity fluid, *J. Fluid Mech.*, *120*, 411–431.

Tobie, G., G. Choblet, and C. Sotin (2003), Tidally heated convection: Constraints on Europa's ice shell thickness, *J. Geophys. Res.*, *108*(E11), 5124, doi:10.1029/2003JE002099.

Tobie, G., G. Choblet, J. Lunine, and C. Sotin (2004), Interaction between the convective sublayer and the cold fractured surface of Europa's ice shell, paper presented at Workshop on Europa's Icy Shell: Past, Present, and Future, Lunar Planet. Inst., Houston, Texas.

Turcotte, D. L., and G. Schubert (1982), *Geodynamics: Applications of Continuum Physics to Geological Problems*, John Wiley, Hoboken, N. J.

Zhong, S. M., M. Gurnis, and L. Moresi (1998), Role of faults, nonlinear rheology, and viscosity structure in generating plates from instantaneous mantle flow models, *J. Geophys. Res.*, *103*, 15,255–15,268.

Zhong, S. M., M. T. Zuber, L. Moresi, and M. Gurnis (2000), Role of temperature-dependent viscosity and surface plates in spherical models of mantle convection, *J. Geophys. Res.*, *105*, 11,063–11,082.

Zimmer, C., K. K. Khurana, and M. G. Kivelson (2000), Subsurface oceans on Europa and Callisto: Constraints from Galileo magnetometer observations, *Icarus*, *147*, 329–347.

A. C. Barr, Department of Earth and Planetary Sciences, Washington University in St. Louis, Campus Box 1169, One Brookings Drive, St. Louis, MO 63130, USA. (amyb@levee.wustl.edu)

R. T. Pappalardo, Laboratory for Atmospheric and Space Physics, University of Colorado, Campus Box 392, Boulder, CO 80309-0392, USA. (robert.pappalardo@lasp.colorado.edu)